A Comparison of Lateral Intention Models for Interaction-aware Motion Prediction at Highways

Vinicius Trentin[a], Antonio Artuñedo[b], Jorge Godoy[c] and Jorge Villagra[d]
Centre for Automation and Robotics, Spanish National Research Council, Madrid, Spain

Keywords: Interaction-aware, Motion Prediction, Lane Change.

Abstract: To safely navigate in complex scenarios is crucial to know the predictions of the vehicles involved in the scene. The future behavior of the traffic participants is dependent on their intentions, the road layout and the interaction between them. In this work, a framework is presented to compute the motion predictions of the surrounding vehicles considering all possible routes obtained from a given map. At each time step, with a Dynamic Bayesian Network, the probability of being on a specific route and the intention to change lanes are computed. Our framework, based on Markov chains, is generic and can handle various road layouts and any number of vehicles. We apply the framework in a two-lane highway and evaluate the influence of different lane-changing methods on the predictions of the vehicles present at the scene.

1 INTRODUCTION

Autonomous vehicles promise to bring many benefits to society, such as low accident rates, safety, fuel saving, better life quality, reduce stress, among others. In order to assure the safety aspect, the algorithms implemented need to deal with a large number of possible scenarios, with a varying degree of complexity, and be able to predict the movement of the other vehicles present in the scene considering their mutual interactions.

The behavior of traffic participants is full of uncertainties in the real world. In order to improve the driving quality, autonomous vehicles should evaluate the threats, should take seriously the ones with high probability to happen and should not overreact to the ones with low probability. Probabilistic intention and motion predictions are unavoidable to accomplish safe and high-quality decision-making and motion planning for autonomous vehicles (Zhan et al., 2018).

In this paper, we propose an approach to compute the motion prediction of the surrounding vehicles in all their possible routes in a short-term horizon. In comparison with a previous work for motion prediction of the same authors sketched in (Medina Lee et al., 2019) and with other works found in the literature, more accurate results are produced here, since this new approach can accommodate restrictions caused by the interaction between vehicles. Since we focus on the lateral interaction, three models for the lateral intention are compared. For the motion prediction, the approach used is compared with two baselines: a set-based motion prediction and a probabilistic prediction considering constant velocity.

This paper is divided as follows: Section 2 presents a short review of some works similar to the one presented in this article. Section 3 described the proposed approach with the lateral models evaluated being presented in Section 4. Section 5 shows some experimental results and Section 6 concludes.

2 RELATED WORK

Since our work is composed of two main building blocks, some of the related work to each part and on the combination of both are presented below.

2.1 Interaction Awareness

Considering that the intention of the other drivers cannot be measured directly, it is necessary to estimate it.

Klingelschmitt et al. (2016), present a framework for assessing traffic scenes with interaction between

[a] https://orcid.org/0000-0001-5732-3263
[b] https://orcid.org/0000-0003-2161-9876
[c] https://orcid.org/0000-0002-3132-5348
[d] https://orcid.org/0000-0002-3963-7952

Trentin, V., Artuñedo, A., Godoy, J. and Villagra, J.
A Comparison of Lateral Intention Models for Interaction-aware Motion Prediction at Highways.
DOI: 10.5220/0010460701800191
In *Proceedings of the 7th International Conference on Vehicle Technology and Intelligent Transport Systems (VEHITS 2021)*, pages 180-191
ISBN: 978-989-758-513-5

traffic participants. They transform the possible behavior patterns of the vehicles involved into hypotheses and compute the joint probability of each hypothesis by reconstructing the individual probability of each behavior. As a result, they obtain the fully interaction-aware joint probability distribution over all the hypotheses. Their approach grows exponentially as the situation complexity and the number of vehicles involved increase.

Lefevre et al. (2013) implement a Dynamic Bayesian Network to reason about the situations and the risks at intersections on a semantic level. The risk is assessed based on the comparison of the intentions with what is expected from the drivers at a given scenario. They model the expected vehicle's motions based on the road network (stop signs, give away lines), distance to the intersections and previous pose and velocity. The intention to stop is computed based on the previous intention and current expectation. With the intention and the maneuver, the future pose and velocity can be estimated. An evolution of this approach considering also lateral expectations has been recently presented (Villagra et al., 2020).

Although these methods take into account the interdependence between vehicles to find the most probable route combination or if the situation offers risk, they do not include the motion prediction of the traffic participants, as all areas they can reach, which is crucial when planning the ego vehicle trajectory.

2.2 Motion Prediction

Althoff and Magdici (2016) propose the use of set-based predictions with reachability analysis to find all possible reachable sets based on a given map and the positions and velocities of the traffic participants. Although this approach ensures a safe planning for the ego vehicle, given that all vehicles follow the traffic rules, it is too conservative and given a complex scenario with many vehicles, the ego vehicle might have to come to a full stop since all paths are occupied.

In another work, Althoff (2010) abstracted the motion model into Markov chains using reachability analysis. He considers the vehicle's dynamics, their mutual interactions (only based on the road geometry and traffic rules) and also the limitation of driving maneuvers due to road geometry, resulting in crash probabilities for the possible paths of the ego vehicle.

In Zechel et al. (2019), the authors present an approach to compute the motion predictions of the vehicles, without prior knowledge of the scene, considering separately the lateral and longitudinal movement. The longitudinal over-approximation is based on intervals obtained from real data. The lateral over-approximation is computed with the use of acceptance distributions where it evaluates all considered lateral accelerations for one specific driver influence, such a static or dynamic obstacle. They compare their approach with the occupancy predictions computed with SPOT and the comparison showed that the occupancy area size could be reduced up to 70% for a prediction horizon up to 1.3 s without errors.

Although these methods can predict the motion of the surrounding vehicles, they can have low accuracy in complex situations involving many vehicles, such as an intersection, due to their interdependent intentions and resulting actions.

2.3 Motion Prediction with Interaction Awareness

As already mentioned, in order to have a better estimation of the future positions of the vehicles involved in the scene, the motion prediction and the interaction awareness should be jointly considered.

Schulz et al. (2018) use a Dynamic Bayesian Network with a particle filter to evaluate the interaction between vehicles and estimate their route and maneuver intentions. From these intentions, an action, represented by an acceleration and yaw rate values, is obtained and the motion prediction is computed. This method considers only the most probable action for the whole time horizon of the prediction, which, in complex scenarios, may negatively influence the motion planning search space.

In Koschi and Althoff (2017a), the authors expand their work from Althoff and Magdici (2016) to include the interaction between drivers in their set-based predictions. They do it by comparing vehicles driving on the same lane and removing the unreachable areas of the following vehicles. As a result, the drivable area of the ego vehicle increases, since some previews occupied areas are removed. This approach, however, considers neither intentions nor traffic rules in the predictions.

3 FRAMEWORK FOR INTERACTION-AWARE MOTION PREDICTION

In Figure 1 the flowchart of the work is presented. Each of the building blocks appearing in the figure will be briefly described in the following sections.

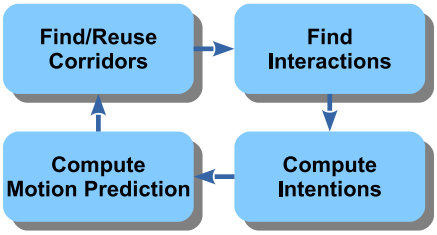

Figure 1: Flowchart.

3.1 Find/Reuse Corridors

Given a map formed by lanelets (Bender et al., 2014), their relational and physical layers are used in order to obtain all the navigable corridors for the vehicles in the scene. The length of these corridors has, at minimum, the distance that the car can reach in a time interval with its current speed, assuming a constant maximum acceleration.

First, we obtain the current lanelet(s) where the vehicle is located, comparing the position and the orientation in the physical layer. Next, a graph search is performed for surrounding lanelets starting from the vehicle lanelet(s) to create a lanelet-sequence for each corridor.

In the next iterations, the corridors found can be either expended or removed, if necessary. The expansion occurs if its predicted occupancy probabilities fall in cells that are farther then a percentage of the grid length (85% in our case). The removal occurs if the current measured orientation of the vehicle has a difference bigger than a threshold when compared with the center line of the corridor.

At each iteration, the lanelet in which the center of the vehicle is located is found. Based on this information, each corridor is defined as being left, center, right or not reachable with respect to the position of the vehicle. To reach the corridors at right/left, a Bézier curve is created that concatenates the two road segments (the one in the current lane with the one in the adjacent lane) with a length of $max(4v, 10)m$, being v the current vehicle's velocity and 4 is the considered duration of a lane change (in seconds). These values were defined after analyzing the patterns of a lane change.

The detection of a lane change is based on the position of the vehicle and occurs in one iteration: at instant t the vehicle is in lanelet x and at instant $t+1$ the vehicle is in lanelet y.

With the exception of the ego vehicle, for each corridor of the other vehicles, a grid is created based on the shape of the road. For the ego vehicle, a route is assumed. An example of the corridors of a vehicle is shown in the Figure 2, where for one of the corridors the grid is drawn.

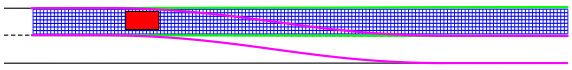

Figure 2: Example of corridors and grid.

3.2 Find Interactions

A search of surrounding vehicles is performed for all the vehicles in the scene, generating a table that contains the distances and velocities.

In order to restrict the motion probabilities in corridors that have another vehicle or that can collide with the corridors of other vehicles, the collision point between these corridors is obtained as can be seen in Figure 3. They result from the intersection between the corridors' center lines, where the chosen point is the first where the distance is less than a given threshold. So far, these types of collisions are not being considered when both vehicles are changing lanes, being this a future work.

Figure 3: Example of collision between corridors.

3.3 Compute Intentions

In order to compute the intention of the traffic participants, the Dynamic Bayesian Network (DBN) proposed by Villagra et al. (2020) is inferred using a particle filter. For each of the vehicles present in the scene, with the exception of the ego vehicle, the network represented in Figure 4 is instantiated, where bold arrows represent the influences of the other vehicles on vehicle n.

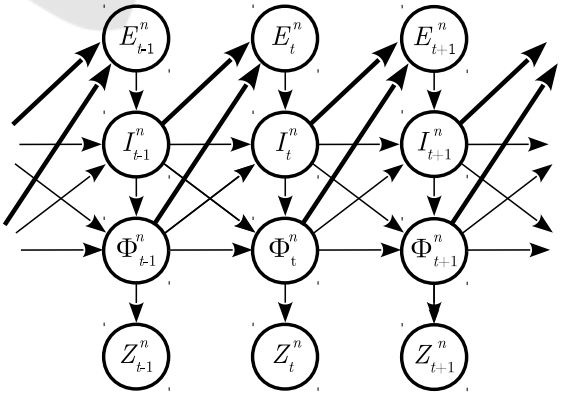

Figure 4: Bayesian network.

The relations among variables appearing in Figure 4 allows to model the driving scene as the following generalized distribution (Lefevre et al., 2013):

$$P(E_{0:T}, I_{0:T}, \Phi_{0:T}, Z_{0:T}) = P(E_0, I_0, \Phi_0, Z_0) \times \prod_{t=1}^{T} \times \prod_{n=1}^{N} [P(E_t^n | I_{t-1} \Phi_{t-1}) \times P(I_t^n | \Phi_{t-1}^n I_{t-1}^n E_t^n) \times P(\Phi_t^n | \Phi_{t-1}^n I_{t-1}^n I_t^n) \times P(Z_t^n | \Phi_t^n)] \quad (1)$$

where the variables are described below:

- Expected maneuver E_t^n: represents the expected lateral behavior of the vehicle n at instant t according to traffic rules. It models the probability that the vehicle can make a lane change without hindering traffic. It can assume two values: *stay* and *change*.
- Intended maneuver I_t^n: represents the intention of the vehicle and includes the route the vehicle intends to follow.
- Physical vehicle state Φ_t^n: represents the pose and speed of the vehicle. They are calculated at each instant based on the intentions.
- Measurements Z_t^n: represents the real measurements of the physical state of the vehicle, extracted directly from exteroceptive sensors of the ego-vehicle or via V2X communications.

3.3.1 Lateral Expectation

The decision to change lanes should be based on the desire to quit the current lane, the selection of the target lane and the feasibility of the change.

Lane changes are usually classified as mandatory or discretionary, depending on the drivers motivation. A Mandatory Lane Change (MLC) is performed when the driver is trying to move his/her vehicle from its current lane into the target lane in anticipation to a left or right exit or a lane closure immediately downstream. A Discretionary Lane Change (DLC) is conducted to improve driving conditions when the driver desires a faster speed, greater following distance, etc. in the target lane Vechione et al. (2018); Toledo et al. (2003).

When implementing the aforementioned particle filter, for every vehicle in every particle the vehicles followers and leaders in all possible lanes are determined and the distances bumper-to-bumper and the velocity differences are found. This information is used to compute the expected lateral motion of the vehicles present at the scene, for which three models were selected, implemented and compared (see Section 4 for more details). Two of these models use only DLC and the third one uses a hybrid approach between MLC and DLC.

3.3.2 Lateral Intention

The lateral intention is computed based on the previous intentions (I_{t-1}) and the current expectation(E_t). The intention will be considered equal to 1 (change lane) if a random value is smaller then the probability generated by Table 1.

Table 1: Lateral Intention.

I_{t-1}	E_t	Probability
0	0	0.1
0	1	0.5
1	0	0.5
1	1	0.9

In this step it is also defined the new corridor of each vehicle in each particle. If the intention is to change, one of the corridors in the target lane defined in the previous step is selected.

3.4 Compute Predictions

To compute the probabilistic predictions of the vehicles present at the scenarios, the library CORA (Althoff, 2015) has been used following the strategy proposed in Althoff (2010). The predictions are computed by abstractions of the system dynamics into Markov chains, where the state space X and input space U are discretized into intervals. The former representing the longitudinal position s and velocity v, each interval with size 0.5 m x 1 m/s, respectively, and the latter representing the acceleration a normalized into [-1, 1].

The longitudinal vehicle's dynamics are expressed using the following differential equation:

$$\dot{s} = v$$
$$\dot{v} = \begin{cases} a^{max} u, & 0 < v < v^{sw} \cup u \leq 0 \\ a^{max} \frac{v^{sw}}{v} u, & v > v^{sw} \cap u > 0 \\ 0, & v \leq 0 \end{cases} \quad (2)$$

where a^{max} is the maximum acceleration allowed, v^{sw} is a switching velocity that changes the acceleration dynamics, and u is the input ranging from -1 to 1.

For the lateral dynamics, it is assumed that the vehicle can occupy the entire lane width with a constant standard deviation.

The transition probability matrices of the Markov chains for a time step $\Phi(\tau)$, and for a time interval $\Phi([0,\tau])$, where τ is the time increment, are computed offline with reachability analysis that aims to compute an over-approximation of the set of states a system can reach given its initial states, inputs and parameters. For each state of the state space and for each

input of the input space, the motion model is applied for a time interval τ resulting in a set covering one or more cells from the state space. The probability of reaching the cell j, starting from cell i under the influence of input β is computed as follows:

$$\Phi_{ji}^{\beta}(\tau) = \frac{V(R_i^{\beta}(\tau) \cap X_j)}{V(R_i^{\beta}(\tau))} \tag{3}$$

where the operator V returns the volume of the set and $R_i^{\beta}(\tau)$ is the reachable set starting from cell i applying input β. The transition probabilities between the input states are represented by the input transition matrix $\Gamma(t_k)$. This matrix is composed by two parts: a transition matrix Ψ, which models the intrinsic behavior of the vehicle when there are no priorities for certain input values, and a priority vector λ, representing the restrictions caused by the road layout, the interaction with other vehicles or a combination of both. A detailed explanation of these variables can be found in Althoff (2010). These parts are joined as follows

$$\begin{aligned} \Gamma_i^{\beta\delta} &= norm(\hat{\Gamma}_i^{\beta\delta}) \\ \hat{\Gamma}_i^{\beta\delta} &= \lambda_i^{\beta}\Psi^{\beta\delta}, \forall i : \sum_{\beta}\lambda_i^{\beta} = 1, 0 \leq \lambda_i^{\beta} \leq 1 \end{aligned} \tag{4}$$

to form the transition matrix where i is the index of a state space and β and δ are indices of two possible input states. The reason this matrix is not joined into the transition matrix $\Phi(\tau)$, is that the priority vector λ can change at each step.

The probabilities distribution for future time steps $p(t_{k+1})$ and time intervals $p(t_k, t_{k+1})$ are computed as follows:

$$\begin{aligned} p(t_{k+1}) &= \Gamma(t_k)\Phi(\tau)p(t_k) \\ p(t_k, t_{k+1}) &= \Phi([0,\tau])p(t_k) \end{aligned} \tag{5}$$

For each corridor from each vehicle a Markov chain is instantiated and the predictions are computed for a time interval. These predictions are multiplied with the sum of the weights of the particles that contains the corridors and they are later joined into a single grid based on the ego-vehicle position, whose size is based on the ego-vehicle's velocity and the situation context.

4 LATERAL MODELS

The models implemented and compared are presented below. These models were selected based on their simplicity and low computational cost.

4.1 Model 1

The first model implemented is based on Mathew (2019). The desire to change lane is computed by the deceleration a provoked by the leading vehicles (when they exist) traveling in front of each vehicle in the current and adjacent lanes:

$$a = \frac{\rho v^m \Delta v}{\Delta x^l} \tag{6}$$

where v is the velocity of the vehicle, Δv is the difference between the velocities of the vehicle and the one of the leading vehicle, Δx is the distance between vehicles and ρ, m and l are parameter models. With the acceleration values a_i in each of possible lanes, the utility U_i of each lane i is defined as:

$$U_i = \frac{e^{a_i}}{\sum_{j=1}^{N} e^{a_j}} \tag{7}$$

where a_i is the acceleration with respect to the leading vehicle of lane i and N is number of possible target lanes.

If the leading vehicle in the current lane is making the target vehicle brake, the lane with the highest utility is selected, otherwise, a random lane, among the possible lanes, is selected.

Once the lane is selected, it is necessary to verify that the deceleration imposed to the new follower, computed with (6), is below a given threshold b, such that $a > -b$.

If the safety criteria is met, the probability to accept the gap is computed as:

$$\begin{aligned} P(lead) &= 1 - e^{-\lambda(t_{lead} - \tau)} \\ P(lag) &= 1 - e^{-\lambda(t_{lag} - \tau)} \end{aligned} \tag{8}$$

where t_{lead} and t_{lag} are the time gaps with respect to the leading and following vehicle in the target lane.

The probability to change lane is the result of the multiplication of $P(lead)$ and $P(lag)$ and the expected lateral movement will be 1 if this probability is bigger than a random value.

4.2 Model 2

The second model implemented is the Minimizing Overall Braking Induced by Lane Changes (MOBIL) (Kesting et al., 2007), used in combination with the Intelligent Driver Model (IDM) (Treiber et al., 2000).

As in the previous model, this one also includes a safety criteria: the deceleration of the new follower a_{nf} in the target lane, after the lane change, cannot exceed a given safety limit b_{safe}

$$a_{nf} > -b_{safe} \tag{9}$$

The authors of MOBIL propose two types of incentive criterion for lane changing: one considering symmetric passing rules and an asymmetric one. The one adopted in this work is the asymmetric model, where the right most lane is the default lane and the lanes on the left should only be used for overtaking purposes.

The incentive criterion for a lane change to a left (L) lane and to a right (R) lane are:

$$\begin{aligned} L &= \tilde{a}_c - a_c + p(\tilde{a}_n - a_n) > \Delta a_{th} + \Delta a_{bias} \\ R &= \tilde{a}_c - a_c + p(\tilde{a}_o - a_o) > \Delta a_{th} - \Delta a_{bias} \end{aligned} \tag{10}$$

where $\tilde{a}_c$, a_c, $\tilde{a}_o$, a_o, $\tilde{a}_n$ and a_n are the accelerations of the target vehicle, old follower and new follower after and before the lane change, p is the politeness factor, Δa_{th} and Δa_{bias} are the acceleration threshold and bias, respectively. It can be noticed that the lane change to a right lane considers only the advantages to the old follower. A lane change to a left lane, on the other hand, takes into account the effects caused to the new follower. The politeness factor p determines how much the others vehicles influence the lane-changing decision of the target vehicle.

The IDM acceleration of each vehicle α depends on the distance s_α and on the velocity difference Δv_α to the leading vehicle. It is composed of two parts: the acceleration $a[1-(v_\alpha/v_o)^4]$ on a free road and the braking $-a(s^*/s_\alpha)^2$ caused by a leading vehicle.

$$\begin{aligned} \dot{v}_\alpha &= a\left[1-\left(\frac{v_\alpha}{v_o}\right)^4 - \frac{s^*(v_\alpha,\Delta v_\alpha)^2}{s_\alpha}\right] \\ s^*(v,\Delta v) &= s_o + vT + \frac{v\Delta v}{2\sqrt{ab}} \end{aligned} \tag{11}$$

where a is the maximum acceleration, b is the desired comfortable deceleration, s_o is the minimum distance, v_o is the desired velocity and T is the safe time gap.

4.3 Model 3

The third model implemented is based on Toledo et al. (2005). The authors argue that the classification of the lane changes into MLC or DLC does not allow the capture of trade-offs between the two types. For this reason, they created a method that includes both types in a single model.

This model penalizes the most right lane, since it considers this lane as being of low speed, caused by the entrances and exits.

At the highest level of the model, the driver chooses a target lane. It is the lane, among all the possible lanes, the driver recognizes as the best lane to be in after considering a wide range of factors and goals. The utilities of the various lanes are given by:

$$\begin{aligned} U_{int}^{TL} = \beta_i &- 0.011D_{int} + 0.119S_{int} + 0.022\Delta X_{int}^{front}\delta_{int}^{adj} \\ &+0.115\Delta S_{int}^{front}\delta_{int} - 2.783\delta_{nt}^{taigate}\delta_{int}^{CL} \\ &+\delta_{int}^{CL} - 2.633\Delta CL_{int} + \beta_i^{path}[d_{nt}^{exit}]^{-0.371} \\ &-0.980\delta_{nt}^{next\ exit}\Delta Exit_i - \alpha_i\nu_n \end{aligned} \tag{12}$$

where U_{int}^{TL} is the utility of lane i as a target lane to the driver n at time t, βi is the lane i constant, D_{int} and S_{int} are the lane-specific densities and speeds, ΔX_{int}^{front} and ΔS_{int}^{front} are the spacing and relative speed of the front vehicle in lane i. δ_{int}^{adj}, δ_{int}^{CL} and $\delta_{nt}^{tailgate}$ are indicators with value 1 if i is the current or an adjacent lane, if i is the current lane, if vehicle n is being tailgated at time t, respectively, lane, 0 otherwise. ΔCL_{int} is the number of lane changes required to get to lane i from the current lane. β_i^{path} is the path plan impact coefficient for lane i, $\delta_{nt}^{next\ exit}$ is the distance to the exit driver n intends to use. $\delta_{nt}^{next\ exit}$ indicates with 1 if the driver intends to take the next exit, $\Delta Exit_i$ are the number of lane changes required to get to the exit lane from lane i. α_i is the parameter of the driver specific random term ν_n.

The target lane is chosen as the lane with the highest utility. The probabilities are given by a multinomial logit model:

$$P(TL_{nt} = i|\nu_n) = \frac{exp(V_{int}^{TL})|\nu_n)}{\sum_{j=TL} exp(V_{jnt}^{TL}|\nu_n)} \tag{13}$$

Once the utilities are computed one has to evaluate the lead and lag gaps, which are defined by the bumper-to-bumper distance between the lead and subject vehicle and the bumper-to-bumper distance between the lag distance and the subject vehicle.

The gap is acceptable if it is bigger than the critical gap:

$$P(G_{nt}^{gd} > G_{nt}^{gd,cr}|d_{nt},\nu_n) = \Phi\left[\frac{ln(G_{nt}^{gd}) - G_{nt}^{gd,cr}}{\sigma_g}\right] \tag{14}$$

where $\Phi[]$ denotes the cumulative standard normal distribution, G_{nt}^{gd} and $G_{nt}^{gd,cr}$ are the gap and the critical gap for vehicle n at time t, referring superscript d to the direction of change (current, left or right) and g to the type of gap (lead or lag).

The critical lead and lag gaps are given by:

$$\begin{aligned} G_{nt}^{lead\,d,cr} &= exp(1.553 - 6.389max(0,\Delta S_{nt}^{lead\,d}) \\ &\quad -0.14min(0,\Delta S_{nt}^{lead\,d} - 0.008\nu_n) \\ G_{nt}^{lag\,d,cr} &= exp(1.429 + 0.471max(0,\Delta S_{nt}^{lag\,d}) \\ &\quad -0.234\nu_n) \end{aligned} \tag{15}$$

$\Delta S_{nt}^{lead\ d}$ and $\Delta S_{nt}^{lead\ d}$ are the relative speeds of the lead and lag vehicles in the direction of change d.

The probability to accept the gap is the result of the multiplication of the acceptance of the lead and lag gap and the expected lateral movement will be to change if this probability is bigger than a random value.

5 EXPERIMENTAL RESULTS

5.1 Scenario

We evaluate the framework proposed in the previous section in a scenario simulated with SCANeR Studio simulator (AVSimulation, 2019). It is a two-lane highway with the ego vehicle (black) and 4 other vehicles (magenta, red, green and yellow), where 4 lane changes are executed. The information about the surrounding vehicles is received by the ego vehicle as a vector of high-level objects containing their estimated pose, velocity, and size. Figure 5 shows the initial position and the path followed by each vehicle and Figure 6 shows the velocities of each vehicle throughout the simulation.

5.2 Execution of the Lateral Models

The simulation is executed three times, one for each lateral model. Figure 7 shows the graphs of expectation and intention for each vehicle with the three models in the simulated scenario, where it can be noticed the specificities of each model. In the expectation of the green vehicle (Figure 7b), once it overtakes the yellow vehicle, the expectation to change lanes from Model 1 stays around 0.5, since no deceleration is caused, meaning both lanes are possible and feasible. For Model 2, the right most lane has always the priority, which can be seen as the expectation stays around 1 when the vehicle is on the left lane and the right lane is available. For Model 3, in the same situation, the expectation is to stay on the current (left) lane, since it penalizes the right most lane and also penalizes lane changes. The penalization to change lanes can be seen in the expectation of the yellow vehicle (Figure 7c) that stays the whole simulation on the right lane and the expectation stays around 0. Since this vehicle is already on the right lane, the expectation for Model 2 stays around 0 and for Model 1 stays around 0.5 when both lanes are feasible.

Figure 8 shows the evolution of the probabilities for each vehicle and each model. These probabilities are computed as $1 - p_{right}$, where p_{right} is the probability of being on the right most corridor. As mentioned before, the probability of each corridor is the sum of the weights of the particles that contains this corridor. Each line, marked with the color of the vehicle on the top right corner, represents the evolution of this vehicle. The x axis is the time and the y axis is the probability of being on each lane, being 0 the right (bottom) lane and 1 the left (top) lane. The line in black is the ground truth, the lane in which the vehicle is at, at each instant. The three models are represented by the lines in red, green and blue, respectively. The magenta dashed line is the orientation of the vehicle withe respect to the orientation of the lane and the numbers mark the lane changes whose leading times for each model are presented in Table 2. The dashed line in blue is the threshold for the detection of a lane change.

Table 2: Leading time.

Lane Change \ Model	1	2	3
1	1.0 s	0.9 s	0.7 s
2	0.8 s	0.8 s	0.9 s
3	0.8 s	0.9 s	0.8 s
4	0.7 s	0.8 s	0.9 s
5	0.9 s	0.7 s	0.6 s
6	1.2 s	1.0 s	1.0 s

5.3 Predictions and Evaluation

Figure 9 shows an example of the predictions computed with the model from Section 3.4 in the last time interval (2.9 - 3.0 s) for all three models. The time when these predictions were made was chosen at 4.6 s, to show an instant where interactions become more intense.

The differences of the models in these figures are more visible in the lane change of the red vehicle. In this particular frame, the intention from the red vehicle to change lanes is more visible in Model 1 than in Model 3, which confirms the differences in the leading time for this lane change (1) in Table 2.

The advantages of the proposed DBN are highlighted when compared with the baselines predictions computed with constant velocity and with the available version of the library SPOT (Koschi and Althoff, 2017b), which produces set-based reachable sets. For the model with constant velocity, the prediction mean and variance used are obtained as follows:

$$\begin{aligned} p(k) &= \mathcal{N}(\mu_k, \sigma_k^2) \\ \mu_k &= x_o + v * k * dt \\ \sigma_k^2 &= k * dt \end{aligned} \tag{16}$$

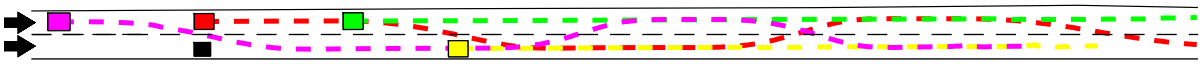

Figure 5: Paths evolution of each vehicle in the simulated scenario.

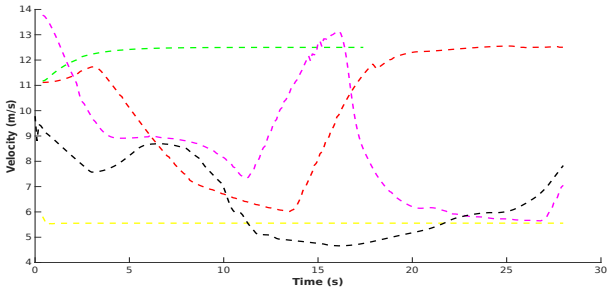

Figure 6: Velocities throughout the execution of the simulation.

The predictions in the time interval 2.9 - 3.0 s for the same time in the simulation for both baseline methods are shown in Figure 10. In the method with constant velocity, both corridors are equally probable and the acceleration history and lane shape are irrelevant: the size of the distribution is the same for all vehicles at every step. The results from SPOT, on the other hand, do include the acceleration's limits and take into account the shape of the road (for the corridors changing lane), but they are too conservative, leaving almost no free space for the motion planning of the ego vehicle.

Figure 11 shows the correlation of the prediction and the actual vehicle pose at the time interval (1.4 - 1.5 s) for all three models. It also includes a numerical evaluation of the prediction at the considered time. The metric used consists in getting the likelihood of the cell the center of the vehicle is located at from a prediction made 1.5 s before. It is one of the criteria used to assess the lateral models behaviour that are compared. Since the red vehicles is the one with the most different values among the models, its evaluation is shown in a zoomed in box on the right of each figure. Table 3 presents the sum of the evaluations for each vehicle for each model for the whole simulation.

Table 3: Evaluation of the predictions per model.

Model / Vehicle	1	2	3
Red	0.34718	0.34871	0.34644
Green	0.22011	0.22223	0.22637
Yellow	0.51265	0.52836	0.52215
Magenta	0.33666	0.34174	0.34041

The vehicles with the more accurate predictions are vehicles that do not change lanes, the green and the yellow (the green vehicle leaves the simulation 10.5 seconds before its end). Besides the early detection of the lane change, it is also due to the fact that the lane changing corridors do not perfectly match the movement executed by the vehicles. Other factor that influences the precision of the prediction is the lateral position of the vehicle within the lane. So far, the lateral distribution is the same for every vehicle, being the mean the center of the lane. The use of an adaptive distribution, considering the lateral displacement of the vehicle is part of a future work.

5.4 Evaluation Metrics

To evaluate the quality of the results, three metrics were defined: the lead time of the detection l, the probability p of being on the current position based on the predictions of a previous time, and the false lane change detection f.

- The lead time l is defined as the time where the corridor that is changing lanes has the biggest priority and maintains the dominance until the lane change is detected.
- The probability p is sum of the evaluation's probabilities for the whole simulation.
- The false detection f is the sum of intervals where the probability is bigger on a corridor that is not the correct one or a noise in the lane change. The intervals between the lead time and the detection of a lane change are not included. One example of a false detection is marked in Figure 8.

Each metric is computed as follows:

$$l_k = \sum_{v=1}^{N} \sum_{c=1}^{Nc_v} l_v^{c^k}, \quad p_k = \sum_{i=1}^{M} \sum_{v=1}^{N} p_v^{i^k}, \quad f_k = \sum_{i=1}^{M} \sum_{v=1}^{N} f_v^{i^k}$$

where $l_v^{c^k}$ is the leading time of the lane change c of the vehicle v for the model k, $p_v^{i^k}$ is the accuracy of a previous prediction at time interval i for the vehicle v for the model k, $f_v^{i^k}$ is the false detection for the vehicle v at the time interval i for the model k, N is the number of vehicles, Nc_v is the number of lane changes for the vehicle v and M is the number of simulated intervals.

Table 4 presents the values of each metric for the three models. For this scenario, model 1 yield better leading times, although the predictions from model 2 and 3 are slightly more accurate. The reason for this is mostly due to the fact that the lane changing corridors do not perfectly match the movement executed by the vehicles. The number of false detection are the same

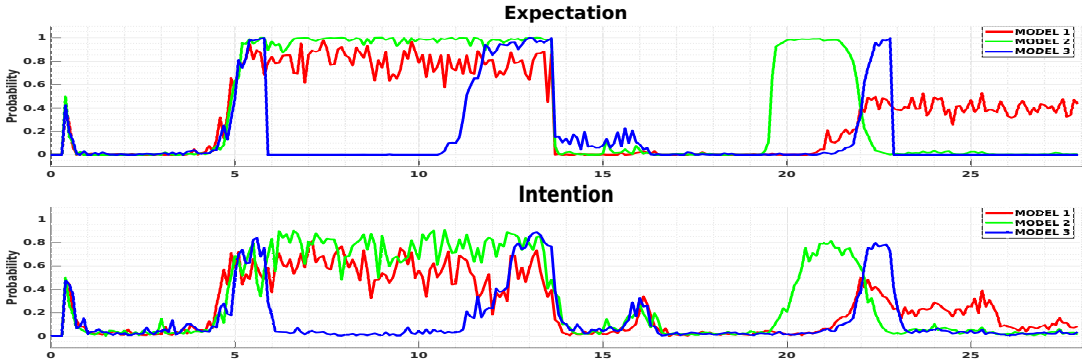

(a) Red Vehicle

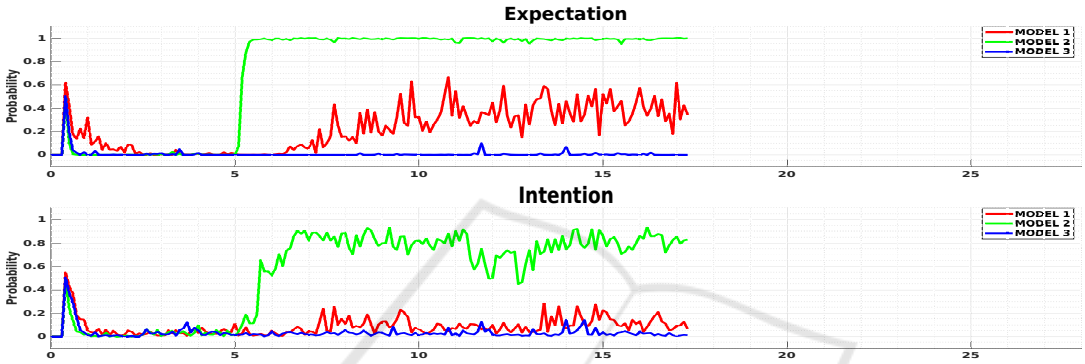

(b) Green Vehicle

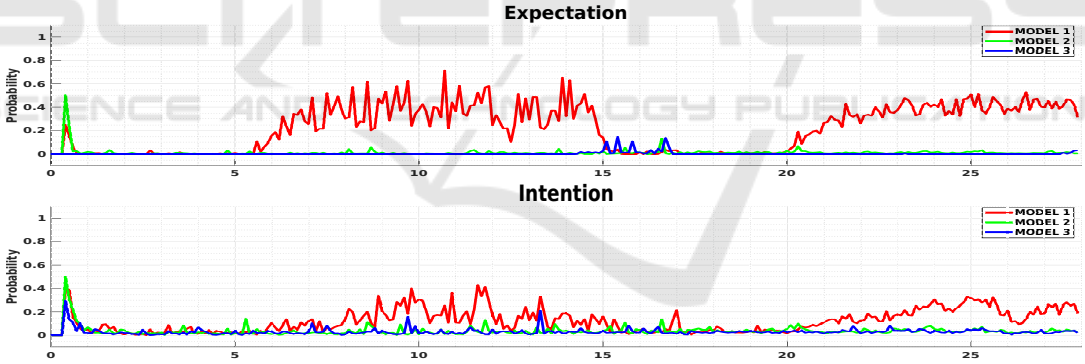

(c) Yellow Vehicle

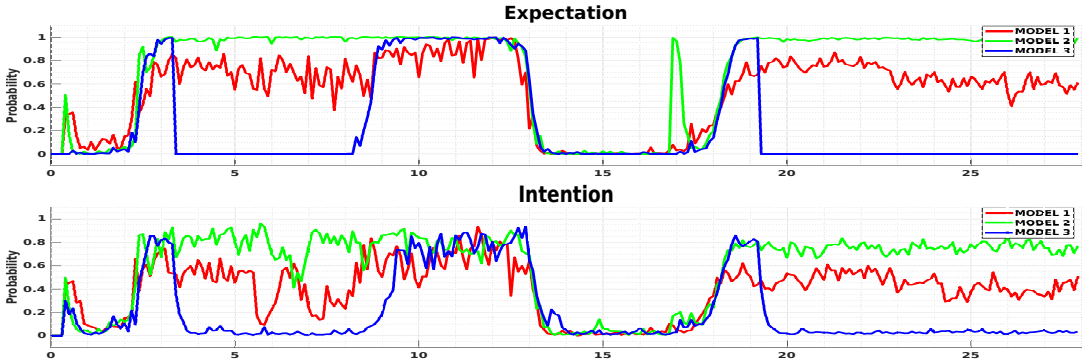

(d) Magenta Vehicle

Figure 7: Expectation and intention for each vehicle.

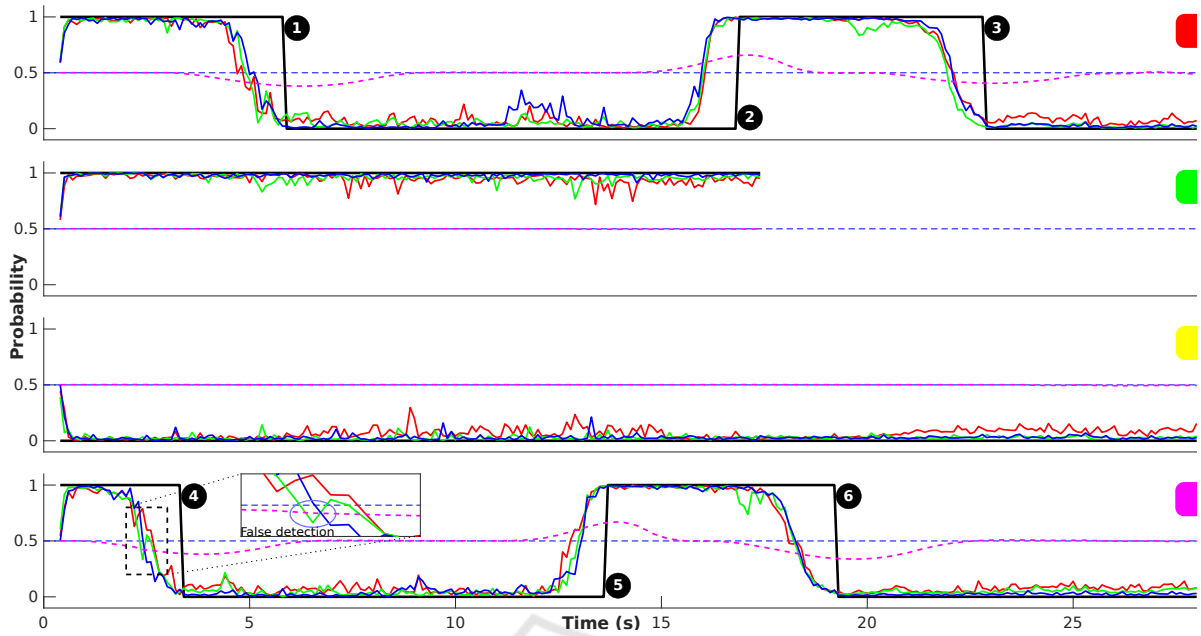

Figure 8: Evolution of each vehicle in the simulation: the line in black is the ground truth; the lines in red, green and blue represent the evolution of the Model 1, 2, and 3, respectively; the blue line is the threshold to identify the lane change; the line in magenta is the orientation of the vehicle with respect to the center line of the lane.

(a) Model 1

(b) Model 2

(c) Model 3

Figure 9: Predictions at the interval 2.9 - 3.0 s for each of the models.

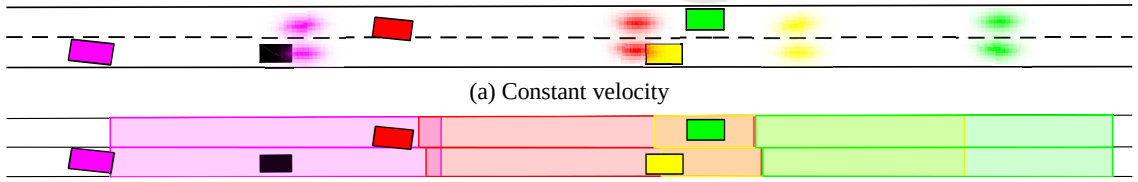

(a) Constant velocity

(b) SPOT

Figure 10: Baseline predictions at the interval 2.9 - 3.0 s.

Table 4: Metrics of each model.

Parameter \ Model	1	2	3
l	5.4 s	5.1 s	4.9 s
p	1.41660	1.44103	1.43536
f	1	1	1

for the three models.

A video with the evolution of the three simulations is available in https://youtu.be/HxXE8bc8-5Y.

We evaluate the three models in another scenario with 3 lanes and 5 vehicles where a higher number of false detection is present. The paths followed by each vehicle and their velocities are shown in Figures 12 and 13, respectively. Due to a lack of space, only the

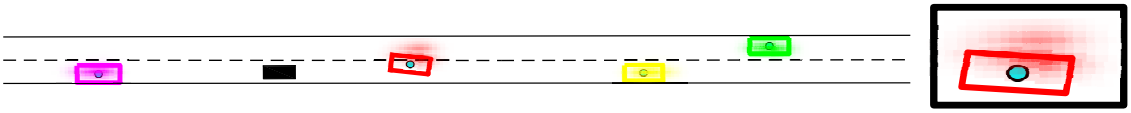

(a) Model 1 - Red : 0.000328 Green : 0.001216 Yellow : 0.001815 Magenta : 0.001189

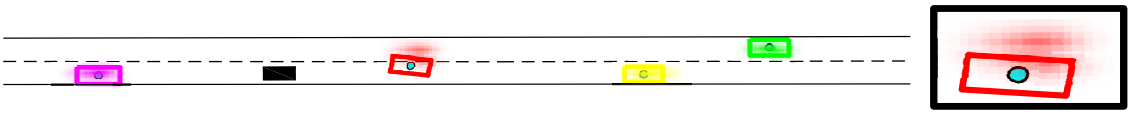

(b) Model 2 - Red : 0.000260 Green : 0.001227 Yellow : 0.001848 Magenta : 0.001207

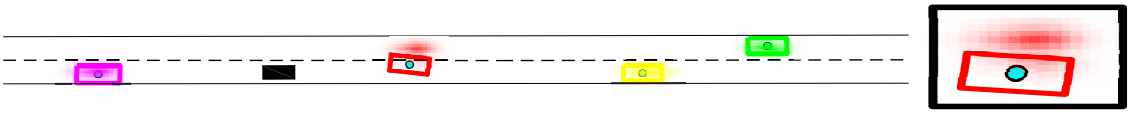

(c) Model 3 - Red : 0.000174 Green : 0.001227 Yellow : 0.001845 Magenta : 0.001191

Figure 11: Evaluation of the predictions.

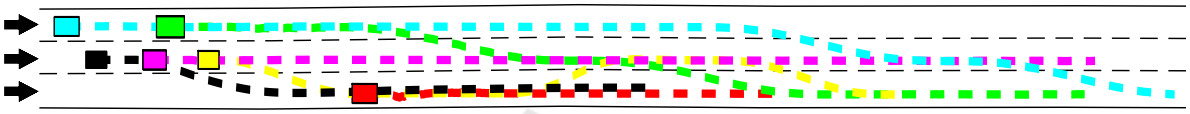

Figure 12: Paths evolution of each vehicle in the second simulated scenario.

result table (Table 5) will be presented.

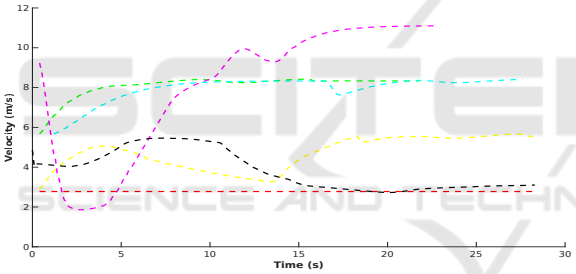

Figure 13: Velocities throughout the execution of the second simulation.

Table 5: Metrics of each model for the second scenario.

Parameter \ Model	1	2	3
l	7.6 s	7.1 s	7.8 s
p	0.9488	0.96688	0.95825
f	71	87	52

In this case, model 3 yield better leading time and the lowest number of false detection. The predictions from model 2 are better but its number of false detection is the highest among the three models.

To combine both experiments, the values of l is normalized by the number of lane changes and the values of p and f are normalized by the number of simulated intervals each vehicle is present and the number of vehicles. Table 6 presents the sum of the normalized results of both simulations for each model.

Table 6: Normalized sum of the results.

Parameter \ Model	1	2	3
l_{norm}	1.9857	1.8643	1.9309
p_{norm}	0.002150	0.002187	0.0021789
f_{norm}	0.0609	0.0732	0.0448

Based on the results from Table 6, for the scenarios evaluated, model 3 produced, in general, better results:

- its normalized false detection is the best among the all models; and
- its normalized predictions are more accurate than the ones from model 1, that has the best normalized leading time; and
- its normalized leading time is better than the one from model 2, that has the best normalized predictions;

6 CONCLUSION AND FUTURE WORK

In this work we present the framework currently being used by the AUTOPIA Group for the motion prediction and interaction-aware of vehicles at highways. Three models for the lane change were implemented and compared. With the metrics used in this work, the model from Toledo et al. (2005) yield better results.

A comparison of the motion prediction with two baseline models was presented. The results from

SPOT, although more accurate, are too conservative, leaving the ego vehicle, in some cases with no or almost no space for the motion planning. The importance of interactions modeled with a DBN is highlighted when compared with the simple model with constant velocity, where all the possible corridors have the same probability and the acceleration input has no influence in the predictions.

As future work, we intend to use the framework presented in more complex scenarios, such as highways with entrances and exits, and use public available datasets.

ACKNOWLEDGEMENTS

This work has been partially funded by the Spanish Ministry of Science and Innovation, the Community of Madrid through SEGVAUTO 4.0-CM (S2018-EMT-4362) Programme, and by the European Commission and ECSEL Joint Undertaking through the Projects NEWCONTROL (826653) and SECREDAS (783119).

REFERENCES

Althoff, M. (2010). *Reachability analysis and its application to the safety assessment of autonomous cars*. PhD thesis, Technische Universität München, Munich, Germany.

Althoff, M. (2015). An introduction to cora 2015.

Althoff, M. and Magdici, S. (2016). Set-based prediction of traffic participants on arbitrary road networks. *IEEE Transactions on Intelligent Vehicles*, PP:1–1.

AVSimulation (2019). Scaner studio user manual.

Bender, P., Ziegler, J., and Stiller, C. (2014). Lanelets: Efficient map representation for autonomous driving. In *2014 IEEE Intelligent Vehicles Symposium Proceedings*, pages 420–425.

Kesting, A., Treiber, M., and Helbing, D. (2007). General lane-changing model MOBIL for car-following models. *Transportation Research Record*, (1999):86–94.

Klingelschmitt, S., Damerow, F., Willert, V., and Eggert, J. (2016). Probabilistic situation assessment framework for multiple, interacting traffic participants in generic traffic scenes. In *2016 IEEE Intelligent Vehicles Symposium (IV)*, pages 1141–1148.

Koschi, M. and Althoff, M. (2017a). Interaction-aware occupancy prediction of road vehicles. In *2017 IEEE 20th International Conference on Intelligent Transportation Systems (ITSC)*, pages 1–8.

Koschi, M. and Althoff, M. (2017b). Spot: A tool for set-based prediction of traffic participants. In *2017 IEEE Intelligent Vehicles Symposium (IV)*, pages 1686–1693.

Lefevre, S., Laugier, C., and Ibanez-Guzman, J. (2013). Intention-aware risk estimation for general traffic situations, and application to intersection safety. *Inria research report*, RR-8379.

Mathew, T. V. (2019). Lane changing models. https://www.civil.iitb.ac.in/tvm/nptel/534_LaneChange/web/web.html. (Accessed on 11/19/2020).

Medina Lee, J. F., Trentin, V., and Villagra, J. (2019). Framework for motion prediction of vehicles in a simulation environment. pages 520–527.

Schulz, J., Hubmann, C., Löchner, J., and Burschka, D. (2018). Interaction-aware probabilistic behavior prediction in urban environments. *CoRR*, abs/1804.10467.

Toledo, T., Choudhury, C., and Ben-Akiva, M. (2005). Lane-changing model with explicit target lane choice. *Transportation Research Record*, 1934.

Toledo, T., Koutsopoulos, H., and Ben-Akiva, M. (2003). Modeling integrated lane-changing behavior. *Transportation Research Record*, 1857.

Treiber, M., Hennecke, A., and Helbing, D. (2000). Congested traffic states in empirical observations and microscopic simulations. *Physical Review E*, 62(2):1805–1824.

Vechione, M., Balal, E., and Cheu, R. L. (2018). Comparisons of mandatory and discretionary lane changing behavior on freeways. *International Journal of Transportation Science and Technology*, 7(2):124 – 136.

Villagra, J., Artuñedo, A., Trentin, V., and Godoy, J. (2020). Interaction-aware risk assessment: focus on the lateral intention. In *IEEE 3rd Connected and Automated Vehicles Symposium*.

Zechel, P., Streiter, R., Bogenberger, K., and Göhner, U. (2019). Over-approximation of the driver behavior as occupancy prediction. In *2019 IEEE 14th International Conference on Intelligent Systems and Knowledge Engineering (ISKE)*, pages 735–742.

Zhan, W., de La Fortelle, A., Chen, Y., Chan, C., and Tomizuka, M. (2018). Probabilistic prediction from planning perspective: Problem formulation, representation simplification and evaluation metric. In *2018 IEEE Intelligent Vehicles Symposium (IV)*, pages 1150–1156.